Available online at www.sciencedirect.com
SCIENCE DIRECT®
Applied Geochemistry 19 (2004) 957–972
Applied Geochemistry
www.elsevier.com/locate/apgeochem

Lead isotope signatures of Holocene fluvial sediments from the Loire River valley

Philippe Négrel*, Wolfram Kloppmann, Manuel Garcin, Denis Giot

BRGM. Avenue C. Guillemin, BP 6009, 45060 Orléans Cedex 02, France

Received 8 May 2003; accepted 20 November 2003
Editorial handling by R.S. Harmon

Abstract

The distribution of Mn, V, Th, Pb and isotopes of Pb in the labile fraction of sediments from a channel infill in the Middle Loire alluvial plain are used to highlight some aspects of the basin evolution over the period from 0 to 10 ka BP. The acid extractable matter (AEM) in the sediment samples is variable in amount and in trace element contents. Iron-Mn oxyhydroxides are the principle trace element carrying phase in the labile fraction and carbonates are a secondary carrier. Vanadium and Pb originate from the weathering of silicates and are used as a silicate erosion rate index in the fluviatile record. Most of the AEM data plot along a general trend between 3 endmembers (basalts, Cretaceous carbonate rocks and granites) in the relationship between $^{207}Pb/^{206}Pb$ and $^{206}Pb/^{206}Pb$. These endmembers have been mixed in various proportions depending on natural Holocene inputs (erosion, volcanic events) or human influences (mining and smelting of ore).

1. Introduction

Numerous factors influence erosion rates and catchment inputs. They include lithology, relief, climate and human history (Meade et al., 1990). Most investigators interpret continental erosion from the composition of the sediment in large rivers (Gaillardet et al., 1999). However, human activities often profoundly modify the sediment yield (Meade et al., 1990; Macaire et al., 1997). It is generally agreed that rivers and streams carry the residual products from chemical and mechanical weathering as sediments, and that about 90% of this load seems to be stored in the alluvium for periods of 10–1000 a (Meade, 1988).

The Loire River, in central France, is 1010 km long and drains an area of 117,800 km^2. The catchment is composed of various lithologies including old plutonic rocks (500–300 Ma), a large volcanic area (20 Ma–3.45 ka BP) in the upstream section, and carbonate deposits (200–6 Ma old) in the central part. In former studies, the authors reported on changes with time in the distribution of chemical species in the present day suspended matter and bed load sediments collected over the period of a hydrologic cycle (i.e. one year) at one site in the middle Loire watershed. Chemical and isotope data suggest that during high flow conditions, suspended matter and the labile fraction of the sediments (acid extractable matter, AEM) are mainly provided by erosion, whereas during low flow conditions, there is less suspended matter and calcite precipitation becomes the dominant process (Négrel and Grosbois, 1999; Négrel et al., 2000; Grosbois et al., 2000; Négrel and Roy, 2002a).

Once the present day mechanisms of trace metal transfer in a drainage basin, such as biological triggering of calcite and hydroxide precipitation (Grosbois et al., 2000), are elucidated, it becomes possible to reconstruct some aspect of the evolution of the Middle Loire basin (Négrel et al., 2002; Négrel and Roy, 2002a). In this paper, the authors use the distribution of acid extractable Mn, V, Pb (cold 0.2N HCl, Négrel et al., 2000) and Pb isotopes from the labile fraction (Négrel and Roy,

* Corresponding author.
E-mail address: p.negrel@brgm.fr (P. Négrel).

0883-2927/$ - see front matter © 2003 Elsevier Ltd. All rights reserved.
doi:10.1016/j.apgeochem.2003.11.004

2002b) of the alluvial sediments in a clayey channel infilling deposited from 11.5 ka BP to the present to discriminate the different sediment sources and compare present day transport mechanisms to those in the past. This allows the impacts of natural processes (erosion, volcanism, etc) and anthropogenic activity on catchment development during the Holocene to be distinguished.

2. Materials and methods

2.1. Sampling site and protocol

The sampling sites are situated in the middle part of the Loire River course (Avaray Valley Fig. 1, Garcin et al., 1999). The part of the drainage basin upstream of the sampling sites represents about 40% of the total Loire catchment and includes the entire silicate dominated basement of the Massif Central and about 25% of the total area of sedimentary rocks (i.e. the Tertiary lacustrine deposits in the Limagne and the Jurassic, Cretaceous and Tertiary lacustrine and marine deposits of the Paris Basin).

In the Avaray Valley, the Loire is incised into Aquitanian (e.g. Lower Miocene) lacustrine limestone and numerous incisions, oxbows and channels related to meander migration have been identified. Five alluvial bodies were investigated (A to E in Fig. 1, Garcin et al., 1999). A core for geochemical analysis (M25B) was extracted from 6.3 m of Holocene sediments in an oxbow infilling. The following description of the core (Fig. 2) is from Garcin et al. (1999), and the ^{14}C ages are from Garcin et al. (1999, 2001):

(j) 6.3–5.4 m: coarse sand,
(i) 5.4–4.9 m: fine to medium micaceous sand,
(h) 4.9–4.7 m: very fine black peat, the base of which is dated as Middle Boreal (8410±70 a BP),
(g) 4.7–3.5 m: black peat, becoming brownish towards the top, containing much ligneous debris and gastropods (6840±70 a BP at 3.58 m). The top of the peat is Middle Atlantic. There is <1% of reworked Mesozoic and Tertiary plant material,
(f) 3.5–2.9 m: black clays, rich in well preserved gastropods, containing ligneous debris, dated as Atlantic,
(e) 2.9–2.7 m: black clays with sparse gastropods and wood fragments (5350±60 a BP at 2.77 m, end of Atlantic). Reworked pollen (<1%) are present throughout,
(d) 2.7–2.2 m: grey to green clays, sparse shelly debris and very rare vegetal debris (Atlantic).
(c) 2.2–1.0 m: compact green clays with blue spots and very sparse gastropod debris (3360±50 a BP at 2.16 m, Subboreal, 2370±50 a BP at 1.65 m, Subatlantic). The proportion of reworked Mesozoic and Cenozoic pollen is 2–3%, greater than below,

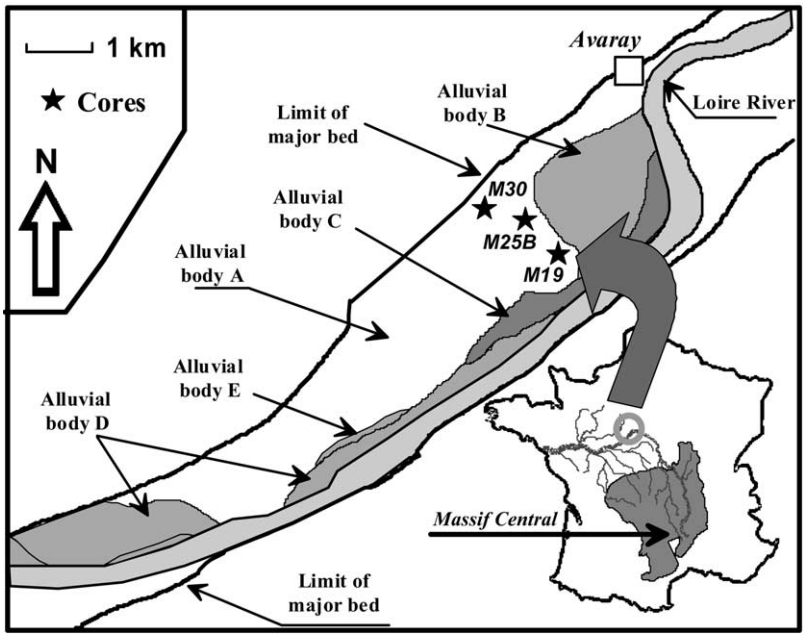

Fig. 1. Map of the Val d'Avaray meander. Numbered core sites are indicated and the schematic cross section shows the meander structure and distribution of sediment bodies A–E (from Garcin et al., 1999).

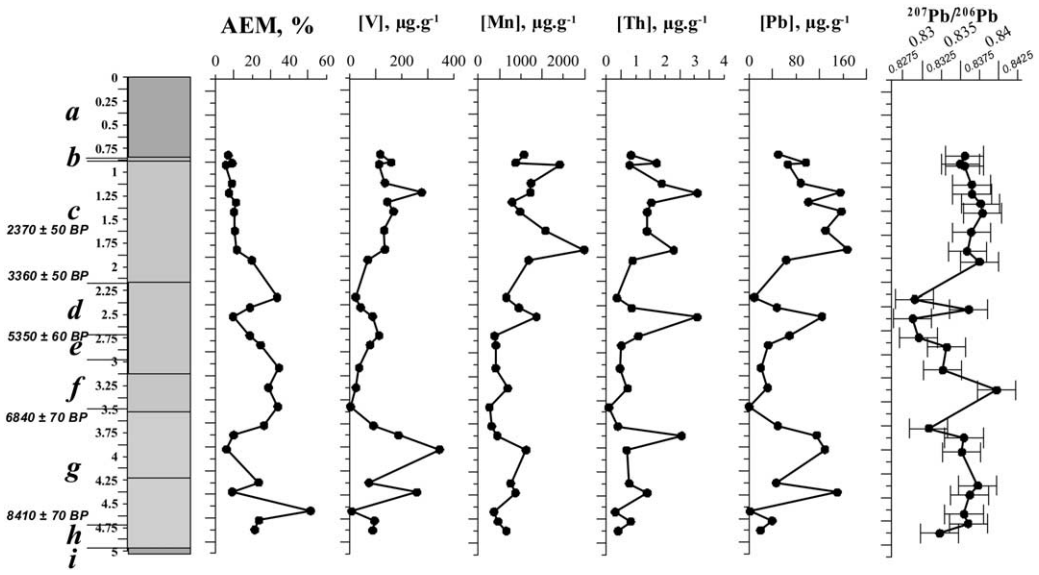

Fig. 2. Lithological log and selected sediment properties in the M25B core. AEM (%), trace elements (V, Mn, Th and Pb in µg g^{-1}) and $^{207}Pb/^{206}Pb$ ratio of the M25B.

(b) 1.0–0.9 m: brownish clays grading into loamy clay,
(a) 0.9–0 m: brown clayey loam and soil.

The channel fill thus spans part of the Boreal, the Atlantic, the Subboreal and probably a large part of the Subatlantic. A peat bog prevailed for approximately 1.5 ka from the Boreal to the Middle Atlantic. Garcin et al. (2001) determined a sedimentation rate of around 0.6 mm a^{-1} from the 15 ^{14}C dates from the core.

Twenty six samples were collected from the core M25B (Table 1), from 0.8 m depth (lower limit of agricultural reworking) to the bottom of the core (6.3 m). Two further samples were collected from a second core (M30, Fig. 1) at a depth of 2.43 m (medium black sand, 11,460±90 a BP, Garcin et al., 1999) and 2.18 m (black clay). A sample of the Aquitanian lacustrine carbonate was collected from a third core (M19) at 5m depth.

Each sample was homogenized by hand-crushing with an agate mortar, then 5 mg of crushed powder were mixed with 3 ml of distilled water and placed on glass slides. Thereafter, the suspensions were dried in air for 3 h. The mineralogical composition of the sediment sample was determined by X-ray diffraction (XRD). Qualitative mineralogical analyses were carried out by identifying diffraction spectra (Brown, 1961). Semi-quantitative percentages were obtained for each mineral by calculating the ratio of the height of its most intense peak against the sum of all the most intense mineral peaks (Hotzapssel, 1985).

2.2. Sample preparation, extraction of trace elements and determination of trace-element and lead isotope measurements

About 20 g of sediments were collected with plastic spatulas and stored in polypropylene boxes (Négrel et al., 2002). After homogenisation with double distilled water, the samples were sieved through a 65 µm nylon mesh and oven-dried at 70 °C. Investigation of the particle size distribution in the sediment (Garcin, unpublish data) shows that 60–97% of the material is represented by the <20 µm (mean 76±14%) fraction, while 14–53% is present in the <4 µm (mean 33±12%) fraction.

Representative aliquots were leached with cold 0.2N HCl to separate a labile fraction (Négrel et al., 2000, 2002; Négrel and Roy, 2002b; Sutherland et al., 2003). This reagent releases the total inventory of non-residual trace elements, i.e. those associated with hydrous Fe–Mn oxides, adsorbed on clays, and occurring in carbonates and sulfides as well as natural organic matter (Chester et al., 1985; Fiszman et al., 1984; Leleyter and Probst, 1999; Sutherland, 2002, Emmanuel and Erel, 2002). The quantity of acid-extractable matter (hereafter referred to as AEM), representing the labile fraction, was determined for each sample by the difference in weight between the initial dried soil or sediment and the residue after the acid extraction and expressed as a percentage of the total matter content (Négrel et al., 2000, 2002; Négrel and Roy, 2002b).

The HCl solution (e.g. of the AEM) was evaporated to dryness, the residue weighed and an aliquot analysed

Table 1
Acid extractable matter (AEM) content of the sediment (mass%) and trace elements (V, Mn, Th and Pb in $\mu g.g^{-1}$) and Pb ($^{207}Pb/^{206}Pb$, $^{208}Pb/^{206}Pb$) isotope ratios in the AEM of samples from cores M25B, M30 and M19

REF	ECH	Depth m	AEM%	V $\mu g\ g^{-1}$	Mn $\mu g\ g^{-1}$	Th $\mu g\ g^{-1}$	Pb $\mu g\ g^{-1}$	$^{207}Pb/^{206}Pb$	$\pm 2\sigma$	$^{208}Pb/^{206}Pb$	$\pm 2\sigma$
M25B/1/53.5	M25B/A	0.80	7	117	1078	0.8	50	0.8356	0.0025	2.0597	0.0062
M25B/2/2.5	M25B/Aa	0.89	9	159	880	1.7	97	0.8350	0.0025	2.0700	0.0062
M25B/2/5.5	M25B/B	0.91	6	112	1913	0.8	66	0.8356	0.0025	2.0717	0.0062
M25B/3/10	M25B/Ba	1.10	9	135	1240	1.9	88	0.8365	0.0025	2.0623	0.0062
M25B/3/20	M25B/C	1.20	7	277	1225	3.1	155	0.8366	0.0025	2.0592	0.0062
M25B/3/30	M25B/Ca	1.30	11	144	798	1.5	101	0.8377	0.0025	2.0685	0.0062
M25B/3/40	M25B/D	1.40	10	168	984	1.4	157	0.8379	0.0025	2.0726	0.0062
M25B/3/60	M25B/E	1.60	11	132	1581	1.4	130	0.8365	0.0025	2.0708	0.0062
M25B/3/80	M25B/F	1.80	12	135	2489	2.3	167	0.8359	0.0025	2.0681	0.0062
M25B/3/91	M25B/Fa	1.91	20	69	1185	0.9	63	0.8376	0.0025	2.0618	0.0062
M25B/5/30	M25B/G	2.30	33	22	658	0.4	9	0.8291	0.0025	2.0470	0.0061
M25B/5/40.5	M25B/Ga	2.41	19	40	954	0.9	47	0.8361	0.0025	2.0700	0.0062
M25B/5/50	M25B/H	2.50	10	87	1368	3.1	124	0.8288	0.0025	2.0484	0.0061
M25B/5/70	M25B/Ha	2.70	19	112	385	1.1	69	0.8296	0.0025	2.0480	0.0061
M25B/5/80	M25B/I	2.80	25	77	418	0.5	33	0.8333	0.0025	2.0632	0.0062
M25B/6/5	M25B/J	3.04	34	35	412	0.5	20	0.8327	0.0025	2.0510	0.0062
M25B/7/25	M25B/K	3.25	29	23	694	0.7	31	0.8398	0.0025	2.0542	0.0062
M25B/7/45	M25B/L	3.45	34	2	267	0.1	0.2	nd	nd	nd	nd
M25B/7/65	M25B/M	3.65	26	90	317	0.4	49	0.8309	0.0025	2.0548	0.0062
M25B/7/75	M25B/Ma	3.75	10	187	448	2.6	115	0.8355	0.0025	2.0668	0.0062
M25B/8/5	M25B/N	3.90	6	346	1124	0.7	129	0.8352	0.0025	2.0635	0.0062
M25B/9/25	M25B/Na	4.25	23	73	762	0.8	46	0.8373	0.0025	2.0622	0.0062
M25B/9/35	M25B/O	4.35	9	258	877	1.4	150	0.8363	0.0025	2.0501	0.0062
M25B/9/55	M25B/P	4.55	52	6	370	0.3	2	0.8355	0.0025	2.0627	0.0062
M25B/9/65	M25B/Pa	4.65	24	94	467	0.8	39	0.8360	0.0025	2.0603	0.0062
M25B/9/75	M25B/Q	4.75	21	88	662	0.4	20	0.8323	0.0025	2.0536	0.0062
M30/2.43	M30a	2.43	21	486	538	1.0	38	0.8323	0.0025	2.0550	0.0062
M30/2.18	M30b	2.18	21	78	582	0.5	44	0.8366	0.0025	2.0647	0.0062
M19/5	M19a	5.00	46	3	346	0.01	0.2	nd	nd	nd	nd

nd refers to non determined values.

for trace elements and Pb isotopes. The concentrations of Mn, Pb, Th and V in the AEM were determined by ICP-MS. Analytical accuracy, measured at better than 10%, was monitored by the repeated analysis of a reference SPEX solution. The concentrations were expressed in μg of element per gram of matter (e.g. the residual product of the acid extraction).

Lead isotopes were determined by ICP-MS measurements on a VG Plasma Quad 2 Plus. Since the earliest work by Hopper et al. (1991), Pb isotope measurements by ICP-MS was largely developed in environmental science; e.g. tracing atmospheric source of Pb (Mukai et al., 1994; Grousset et al., 1994; Monna et al., 1997), identifying the source of Pb in soils (Teutsch et al., 2001; Négrel et al., 2002), investigating the metal dispersal from mining activities (Monna et al., 2000; Mackenzie and Pulford, 2002). The procedure used here was previously described in Cocherie et al. (1998) for Pb isotope measurements in rainwater and the analytical parameters have been optimized for measuring Pb isotopes in sediment leaches. The dead time of the detector is optimised prior to the analyses measuring the $^{208}Pb/^{204}Pb$ ratio of the NIST SRM 981 standard at various concentrations (10, 20, 50 and 100 ppb). The dead time τ is usually comprised of between 20 and 30 ns.

After measurement of the Pb concentration in the samples, the solutions are adjusted to have a concentration of 20 ppb. Similarly, the standard solution is also adjusted to 20 ppb. A bracketing procedure is applied at the same level of counts per second in order to correct instrumental mass bias, according to the following sequence: blank, standard, blank, sample 1, blank, standard, blank, sample 2, blank, etc. Monitoring on ^{208}Pb, a washing time of 3 min is applied after each sample and standard. The ^{204}Hg contribution on 204 peak is corrected using ^{202}Hg with the equation: $^{204}Pb = 204 - (0.23 \times 202)$. The mass discrimination between 202 and 204 masses is neglected as well as the potential $^{186}W^{16}O$ interference on 202 peak, which is supposed to be very unlikely in the samples. ^{187}Re (10 ppb) is used for normalization of blank substraction.

The sample introduction used a "Meinhard" nebulizer allowing the introduction of a flux of 0.3–0.5 ml. min^{-1}. The instrument is used in "peak-jumping" mode with 3 measurements. In order to reduce both the time span on each sample and the potential effect of long term instability and to increase the number of sweeps, the dwell time was changed for each peak as follows: 16 runs of 15 s are recorded allowing good statistics to be obtained in 4 min only. A dwell time of 4, 9, 20, 9, 9 and 4 is respectively applied to masses 187, 202, 204, 206, 207 and 208. Thus, 66 sweeps are achieved in 15 sec.

The internal precision corresponds to the instrumental error or "in-run" error and the external precision or reproducibility is defined as two standard deviations (2σ) of the average values of isotope ratios of repeated analyses of the same sample during various data acquisitions. They are measured on standard NIST SRM 981, a Pb-reference SPEX solution and several samples where concentrations were adjusted. Despite these recent statistical improvements, the same uncertainty as published in Cocherie et al., (1998) was used in this study: e.g. 0.5% for $^{206}Pb/^{204}Pb$ and $^{207}Pb/^{204}Pb$, 0.7% for $^{208}Pb/^{204}Pb$, 0.3% for $^{207}Pb/^{206}Pb$ and $^{208}Pb/^{206}Pb$. The authors recently confirmed these ranges of precision after an intercomparison study (Cocherie, unpublished data) on urban dust using both ICP-MS Quad and MC-ICP-MS directly after dissolution of the material, compared with measurements using MC-ICP-MS and TIMS on a purified aliquot of the same samples.

In earth science, Pb isotopes are generally represented using the non radiogenic isotope ^{204}Pb for normalisation, comparing to the ^{206}Pb, ^{207}Pb and ^{208}Pb which are produced by the radioactive decay of ^{238}U, ^{235}U and ^{232}Th, respectively. In environmental studies, the ratios are usually normalized to ^{206}Pb or ^{207}Pb (Renberg et al. 1994; Monna et al., 1997). Due to the better analytical precision, the $^{207}Pb/^{206}Pb$ and $^{208}Pb/^{206}Pb$ ratios will be used during the course of this work.

3. Results

3.1. Proportion of AEM and its chemical composition

The proportion of AEM ranged from 6% to 52% in the M25B and M30 cores (Table 1) and are similar to those in present day suspended matter of the Loire River (8–47%, Négrel et al., 2000). Semi-quantitative XRD analysis of the sediment showed that quartz, feldspar and calcite are the main mineral components. Quartz and feldspar abundances are higher in the upper part of the core (~10–25% within the interval 0.8–1.8 m), calcite dominates in the intermediate part of the core (~10–40% within the interval 2.3–3.45 m) while clay mineral abundances fluctuate from 25% up to 90% along the core. The clay mineralogy in the <4 μm fraction is dominated by interstratified smectite-illite (40–90%); illite and kaolinite make up the rest of the clay minerals. The positive correlation between calcite and AEM (Fig. 3) indicates that the AEM content is mainly carbonate and the intercept X-axis of the AEM/calcite correlation line shows that the proportion of AEM not derived from carbonate is less than 5%. No clear relationship was observed between AEM and clay mineral content. Iron–Mn oxy-hydroxides (not detected by the XRD analysis) and organic matter could be responsible for some of the largest AEM amounts (see Section 4.2).

From the base of the core to 3.75 m depth the AEM percentage decreases irregularly upwards (Table 1,

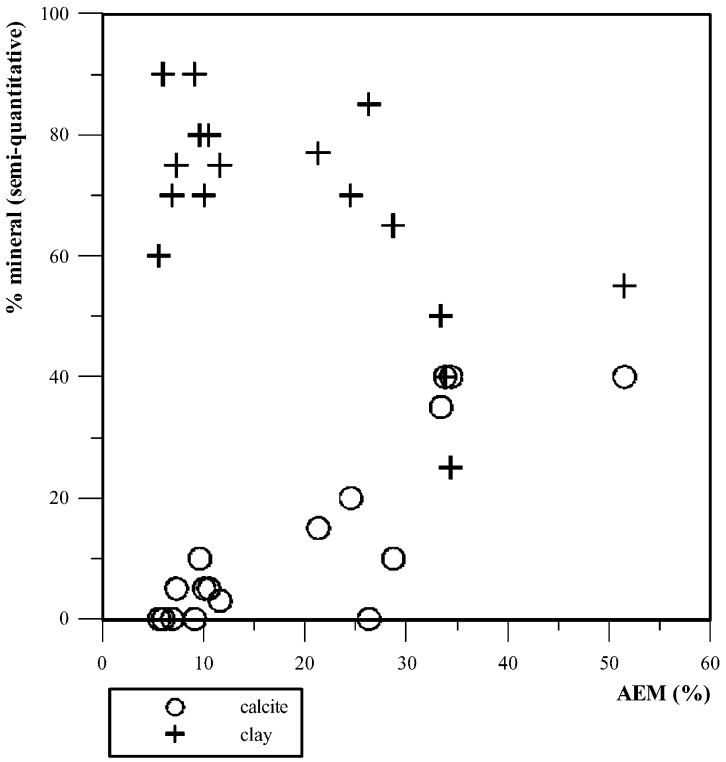

Fig. 3. Relationship between the % of acid extracted matter (AEM) in the sediment and the proportion of calcite and clays (sum of individual mineral amounts) determined by X-ray diffraction analysis.

Fig. 2). Between 3.75 and 2.5 m it increases and then decreases with a maximum of around 34% at a depth of 3.45–3.04 m. From 2.5 m to the top of the core, AEM decreases regularly, finally reaching a minimum of ca. 6–9%.

In the same core, V contents range from 2 to 346 $\mu g.g^{-1}$ (Fig. 2). Low V contents, around 100 $\mu g.g^{-1}$, occur at the base of the peat deposit (4.6–4.8 m) and one of the lowest V values (6.3 $\mu g.g^{-1}$) occurs just above at a depth of 4.5 m. Large fluctuations then occur upcore (4.35–3.45 m) where the highest V content of 346 $\mu g.g^{-1}$ is reached. From 3.45 m to the top of the core the V content increases, although there are some fluctuations. Manganese contents range from 267 to 2489 $\mu g.g^{-1}$, and display a generally increasing trend with several fluctuations from the base to the top of the core. Thorium contents range from 0.1 to 3.1 $\mu g.g^{-1}$ (Fig. 2). Low values occur at the base of the peat deposit (4.6–4.8 m) up to 4.5 m depth. Larger fluctuations then occur upcore and high Th values are reached (2.6 $\mu g.g^{-1}$ at depth 3.75 m; 3.1 $\mu g.g^{-1}$ at depth 2.5 m; 2.3 $\mu g.g^{-1}$ at depth 1.8 m and 3.1 $\mu g.g^{-1}$ at depth 1.2 m).

Samples from the M30 core contain approximately the same Mn (538 and 582 $\mu g.g^{-1}$ at 2.18 and 2.43 m) and Th (0.5–1 $\mu g.g^{-1}$) but have different V contents. The V value at 2.18 m (78 $\mu g.g^{-1}$) is similar to those of the M25B core, but elevated concentrations were recorded at 2.43 m (486 $\mu g.g^{-1}$). A representative sample of the Aquitanian lacustrine carbonate from core M19 (AEM 46%) contains 3 $\mu g.g^{-1}$ of V and 346 $\mu g.g^{-1}$ of Mn and low Th (0.01 $\mu g.g^{-1}$).

3.2. Lead content and isotopic variations

The Pb content of AEM shows large fluctuations within the M25B core (Table 1; Fig. 2). The lowest values (<2 $\mu g.g^{-1}$) at 4.55 m and 3.45 m depth are comparable with those in the Aquitanian lacustrine carbonate from core M19 (0.2 $\mu g.g^{-1}$, Table 1). Higher Pb values occur at various levels and seem to display a covariance with Mn and V. At the base of the core, values around 20–39 $\mu g.g^{-1}$ Pb were recorded before a major increase in Pb content occurs at 4.35–3.75 m depth, with Pb contents exceeding 100 $\mu g.g^{-1}$. Between 3.45–2.30 m depth there are generally low Pb contents though with a peak of 124 $\mu g.g^{-1}$ at 2.5 m. The next peak of Pb content (167 $\mu g.g^{-1}$) is at 1.8 m depth, and from this level to the top of the core there is a progressive decrease to 50 $\mu g.g^{-1}$. Samples from the M30 core have Pb contents in the range 38–44 $\mu g.g^{-1}$, similar to those from the lowest part of the M25B core.

Except for 3 points (0.8398 at 3.25 m depth and 0.8288–0.8296 at 2.50–2.70 m depth), the Pb isotope ratios were fairly constant in the M25B core as exemplified by the narrow range of the $^{207}Pb/^{206}Pb$ values (Table 1; Fig. 2), and samples from the M30 core show $^{207}Pb/^{206}Pb$ ratios in the same range as those from the M25B core (Table 1).

4. Discussion

4.1. Flood sediments

During the Late-glacial and Holocene, the substratum of the Avaray valley, consisting of Aquitanian lacustrine carbonate, was incised by the Loire River (Garcin et al., 1999 and references therein). The channel infill deposits (intersected by the M25B core) represent a sediment trap covering at least 8.5 ka. The channel fill seems to consist mainly of fine clayey sediments deposited during flooding of the river as evidenced by the distribution of the particle size ($76 \pm 14\% < 20$ μm, Garcin, unpublished data). Moreover, there is a total absence of coarse clastics and sandy material in the M25B core except in the lower part (interval 6.3–4.9 m, Garcin et al., 1999).

In the present day suspended matter in the Loire River, the proportion of AEM related to the discharge of the river suggests (Négrel et al., 2000) two types of suspended matter. They correspond to seasonal changes; one type represents high flow conditions in winter and the other type represents low flow conditions in summer. During high flow conditions, the AEM is mainly related to erosion products, as indicated by the mineralogy of the suspended matter which consists chiefly of quartz, K-feldspar and plagioclase derived from weathering of the silicate basement in the Massif Central (Négrel and Grosbois, 1999). Conversely, during low flow conditions, a rise in calcite contents in the AEM corresponds to a period of the hydrologic cycle when $CaCO_3$ precipitation is dominant (Négrel and Grosbois, 1999).

Each sample analysed during this study covers several years of deposition and should contain authigenic $CaCO_3$ (dominant in summer) as well as detrital material (dominant in winter). The detrital material is provided by mechanical erosion of the river catchment area. The source of authigenic material such as calcite or Fe-Mn coatings on silicate particles can be local, i.e. in situ precipitation within the channel, but authigenic material may also be created upstream and then transported as coatings on detrital particles (Robinson, 1993).

4.2. Crustal indicators vs. reactive elements in AEM

In many sediments deposited in oxygenated waters, V adsorbs onto both Fe and Mn oxyhydroxides (Wehrli and Stumm, 1989; Sposito, 1989) and onto organic matter (Sposito, 1989). This is particularly true for ferromanganese nodules (Calvert and Piper, 1974) formed in recent sediments deposited on various oceanic margins (Morford and Emerson, 1999). Recently, Schiller and Mao (2000) showed that dissolved V originates from weathering of silicate bedrock, leading to a correlation between V and dissolved Si in river water. The V and Mn contents in the Loire sediments are both negatively correlated with AEM (Fig. 4a and b). It is important to note that the sample from 2.43 m depth in the M30 core has a surprisingly high V content. The relationships between these elements and AEM can be explained by mixing of two endmembers, one of which is a carbonate relatively poor in V and Mn. The V and Mn contents of the Aquitanian lacustrine carbonate correspond to this potential endmember. The second endmember is rich in V and Mn but poor in AEM and could correspond to an oxide and organic matter reservoir. Shiller and Mao (2000) demonstrate that V in river water is correlated with U and Rb, all 3 elements being derived from silicate weathering. Rubidium, known as soluble (Gaillardet et al., 1997) is a crustal tracer in the labile sediment fraction, e.g. derived from silicate weathering and erosion (Négrel et al., 2000, 2002). In the Loire sediment samples, V and Rb contents are strongly correlated ($r = 0.85$, Négrel et al., 2002), the lowest Rb and V contents occurring in the lacustrine carbonate endmember. This correlation suggests a silicate source for these elements, such as the basement of the Massif Central.

Another notable argument concerns Th which displays mostly insoluble behaviour in hydrosystems and is largely concentrated in sediments in the detrital minerals (Aiuppa et al., 2000). The small amount of dissolved Th (i.e. < 0.04 ng.g^{-1} in natural waters, summary in Langmuir and Herman, 1980) shows a strong tendency to be strongly adsorbed onto clays and oxyhydroxides (Langmuir and Herman, 1980). Négrel and Roy (2002b) synthesised the relationship between Rb and Th in AEM from two small watersheds, one on granite-gneiss and the other one on basalts. Although Th and Rb contents fluctuate widely in sediment leaches, they defined the mixing between granite and basalt-derived AEM. Comparing the two watersheds, Th tends to be more enriched in basalt-derived AEM than in granite ones. This discrepancy should reflect the geology of the watershed and the amount of Th–Rb-rich phases in sediments developed over granite. Furthermore, in the present-day AEM in the suspended matter from the Loire River (Négrel et al., 2000; Négrel and Roy, 2002a), the most concentrated samples in Th and Rb, corresponding to high flow conditions, plot within the granite-basalt mixing field. This led to the suggestion that a probable source of elements is from the Massif Central with subsequent transport by the Loire and

tributaries as Fe–Mn oxide coatings on silicate particles mainly provided by erosion. In present-day AEM, the Rb *vs.* Th relationship reveals a linear trend towards a low-Rb/low-Th endmember corresponding to a carbonate endmember which induces a "dilution" of the Fe–Mn coatings (Négrel and Roy, 2002a). This end-member is a mixture of present-day authigenic calcite the neoformation of which becomes dominant during low flow conditions (Négrel and Grosbois, 1999; Négrel et al., 2000) and detrital calcite derived from the erosion. However, Th (and V) vs. Pb relationship shows a different slope, with Pb being hugely enriched in present day AEM as a result of anthropogenic inputs along the Loire River catchment, as stated by Grosbois et al. (2000), Négrel et al. (2000) and Négrel and Roy (2002a).

The comparison between Th vs. Rb contents in the Loire sediments (Fig. 6a) yields a strong correlation with a r coefficient close to 0.78. As for the Rb vs. V relationship (Fig. 5) the lowest Th and Rb contents occur in the lacustrine carbonate endmember and once again this correlation suggests a silicate source for these elements, such as the basement of the Massif Central.

Lead is known to be quite reactive and to adsorb onto solid matter (e.g. suspended matter, soils and sediments); Dong et al. (2003) applying selective extraction techniques on solid phases from Cayuga Lake (USA) found that the greatest contribution to total Pb binding to the surface coating materials was from Mn oxides. In the Loire sediments, V is strongly correlated with Pb (Fig. 5) as are Pb and Th (Fig. 6b), the lowest concentrations of both occurring in the Aquitanian lacustrine carbonate. The relationships between AEM and trace elements and between certain trace elements themselves suggest that V and Pb (as well as Th and Rb) originate from weathering of silicates and therefore can be used as a silicate weathering index in the past fluviatile record. Further constraints on weathering will be added using Pb isotopes (see below).

4.3. Evaluation of sediment sources from lead isotopes

Lead concentrations are often determined in sediments or in separate fractions (bound onto carbonates, oxides etc, Emmanuel and Erel, 2002). However, its concentration alone may not be sufficient for separating pollution from the natural backgrounds as these often vary due to natural processes (e.g. Monna et al., 1999). Variations in the Pb isotope ratios generally reflect the mixing of several sources of Pb with differing isotopic signatures (Monna et al., 2000; Teutsch et al., 2001; Négrel and Roy, 2002; Outridge et al., 2002). Thus combination of both concentrations and Pb isotope ratios may allow differentiation of various Pb source (Hansmann and Köppel, 2000; Hinrichs et al., 2002; Renberg et al., 2002). Fig. 7 shows the relationship between $^{207}Pb/^{206}Pb$ and Pb content, the latter being shown in log-scale for ease of viewing. With coordinates of Pb isotope ratios and Pb contents, mixtures of two components having different isotope ratios and Pb contents yield a hyperbola as a mixing curve (Faure, 1986).

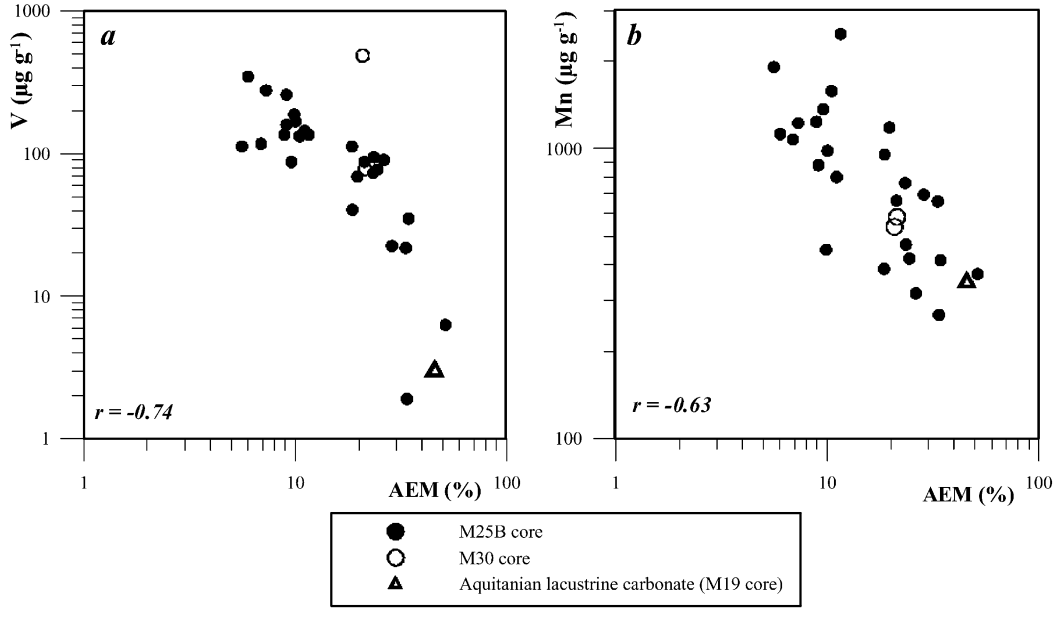

Fig. 4. Relationship between V (black circles) and AEM (%) and Mn (black squares) and AEM (%) in the M25B core (Fig. 4a and b, respectively). Two samples from the M19 core (V: open circles, Mn: open square) and the sample from the Aquitanian lacustrine carbonate from the core M30 (V: open triangle, Mn: open diamond) are also shown.

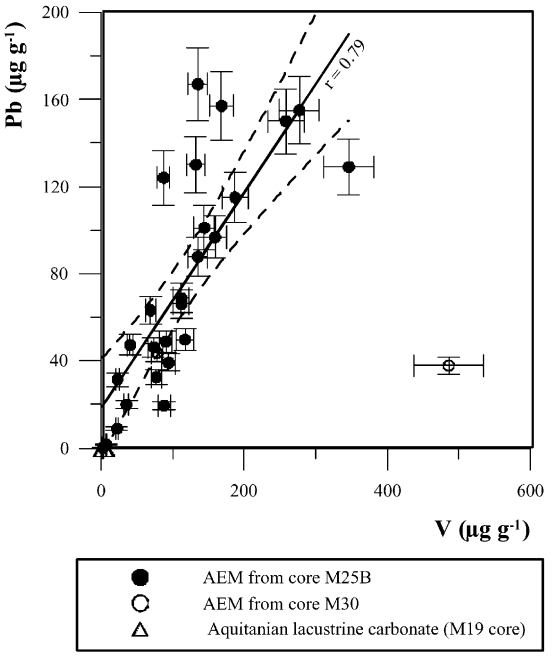

Fig. 5. Relationship between V and Pb in AEM from core M25B (black circles). The linear regression analysis was performed with XLSTAT (Addinsoft, www.xlstat.com), regression line and plot of 95% confidence interval envelopes are indicated. Two samples from the M19 core (open circles) and one from the Aquitanian lacustrine carbonate from core M30 (open triangle) are also shown.

The depiction of such diagrams requires the characterisation of endmembers as Pb sources (Hinrichs et al., 2002; Renberg et al., 2002). In the samples from the Holocene sediment record, Pb originates primarily from the weathering of silicates as they constitute most of the basement in the investigated part of the Loire catchment; the Pb contribution from carbonates only dilutes the crustal signature.

The two potential crustal endmembers, which act as the main sources of Pb, are granites and basalts of the Massif Central (Fig. 1). Analyses of acid-leached K-feldspars and plagioclases from the granites (Michard-Vitrac et al., 1981; Downes et al., 1997) and of granitic whole rock (Downes et al., 1997) yielded isotope ratios of $^{207}Pb/^{206}Pb$ and $^{208}Pb/^{206}Pb$ varying between 0.8405–0.8630 and 2.0861–2.1141, respectively. Analyses of whole rocks yielded total Pb contents ranging from 35 to 60 $\mu g.g^{-1}$ (Downes et al., 1997). Lead-isotope compositions were determined in AEM derived from soil and sediment along two small rivers located in the Massif Central, one flowing from basalt, the other one on granite-gneiss (Négrel and Roy, 2002a, b). On the granitic terrain, Pb originates from natural input through granite weathering and influence of mineralization, giving a Pb isotope composition in the range of the source rocks and a large fluctuation in Pb content (Négrel and Roy, 2002b). This is clearly reflected in Fig. 7 with the larger Pb contents observed in AEM derived from this catchment.

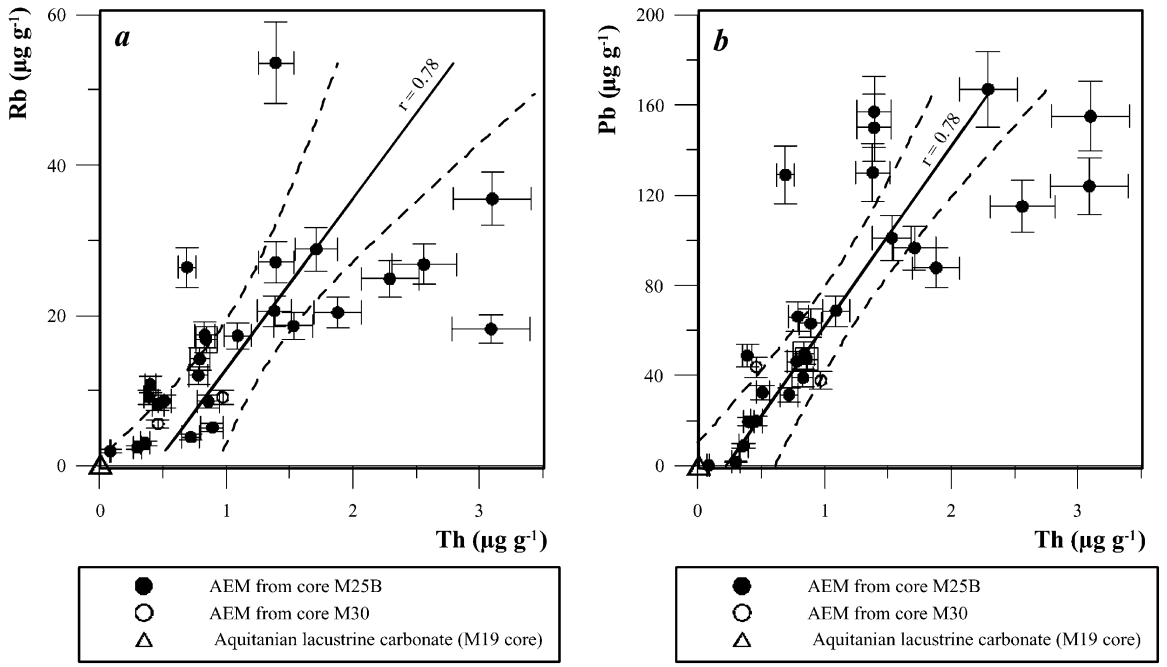

Fig. 6. Relationship between Th and Rb in AEM from core M25B, M19 and M30 cores. Symbols and references for the regression analysis as in Fig. 5.

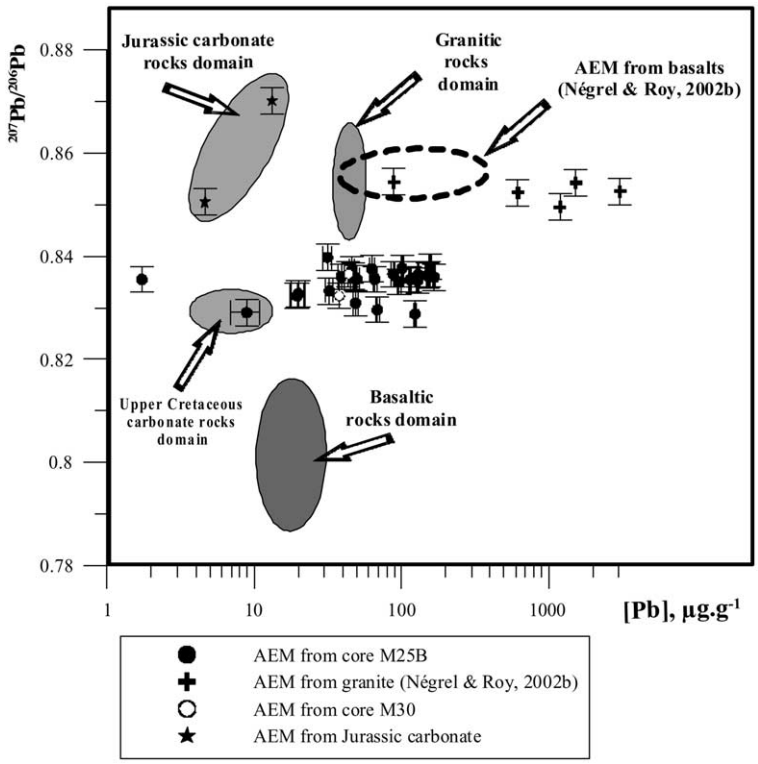

Fig. 7. Relationship between $^{207}Pb/^{206}Pb$ ratio and the Pb content (µg.g^{-1}) from core M25B. The shaded fields represent the various basement rocks from the Loire catchment. The dashed field represents the Pb isotope and Pb content data in the acid extracted matter in soil and sediment from a basalt watershed (Négrel and Roy, 2002b).

Lead isotope ratios on whole rock basalt samples (D. Briot, pers. comm.) fall in the range 0.7890–0.8147 ($^{207}Pb/^{206}Pb$) and 1.9921–2.0422 ($^{208}Pb/^{206}Pb$), and Pb contents are in the range 10–30 µg.g^{-1}. Data on the basaltic watershed, given by Négrel and Roy (2002b), do not plot however within the basaltic rock field because of a modern anthropogenic Pb source related to atmospheric deposition and deriving both from past mining waste and from gasoline inducing a Pb isotope composition similar to granites. Such an atmospheric impact onto soils and sediments is now well constrained, as several workers have shown (Shotyk et al., 1998; Hansmann and Köppel, 2000; MacKenzie and Pulford, 2002).

As the Loire River flows from the silicate basement rocks (basalts, granite and gneiss) to the lacustrine carbonate deposits in the Limagne and marine Jurassic and Cretaceous deposits of the Paris Basin (BRGM, 1996), all these carbonate deposits could be a possible source of AEM. Lead isotope results for the Jurassic deposits (Roy, 1996; Luck and BenOthman, 1998; Négrel, unpublished data) all display high $^{207}Pb/^{206}Pb$ values (0.85–0.87), and Pb contents are lower than 20 µg.g^{-1}. Lead isotope results for the Upper Cretaceous deposits (Roy, 1996; Luck and BenOthman, 1998) all display $^{207}Pb/^{206}Pb$ values around 0.83 and a Pb content in the same range as for the Jurassic deposits. The last carbonate endmember might be linked with carbonate from the Aquitanian or Limagne lacustrine deposits, but there are no Pb isotope data available for these deposits. However, the very low Pb content in these carbonates (around 0.2 µg.g^{-1}) precludes a large role in the Pb budget.

It is obvious from these ranges, also shown in Fig. 7, that all Pb data are scattered between the 3 major endmembers. The granites may correspond to one endmember ($^{207}Pb/^{206}Pb = 0.8405–0.8630$) and it is worth noting that the Pb content in granite-derived AEM is enriched when compared to whole rock ones (Négrel and Roy, 2002b). Basalts may correspond to another endmember ($^{206}Pb/^{204}Pb = 0.7889–0.8147$) and the Pb content in basalt-derived AEM should also be enriched as for granite. The third endmember is Pb-poor and corresponds to the AEM-rich part of the M25B core, suggesting that it originates in carbonate; the Upper Cretaceous carbonates ($^{206}Pb/^{204}Pb$ around 0.85; low Pb content) could play a role, however minor, in the mixing model. The influence of the Jurassic carbonates seems to be negligible.

Fig. 8 is a plot of $^{207}Pb/^{206}Pb$ vs. $^{208}Pb/^{206}Pb$ ratios in the AEM from the M25B core and from granite (Négrel

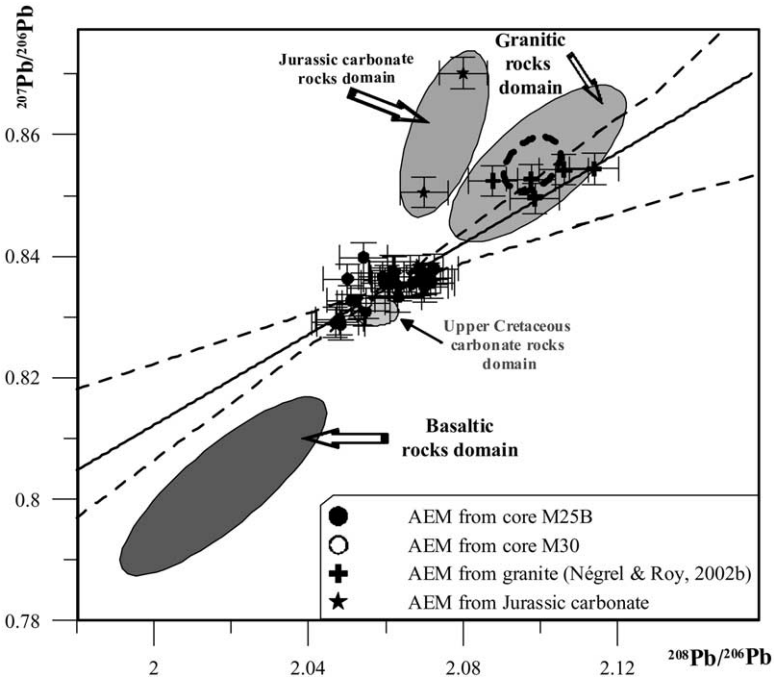

Fig. 8. Relationship between $^{207}Pb/^{206}Pb$ and $^{208}Pb/^{206}Pb$ in AEM from core M25B. The shaded fields represent the various basement rocks from the Loire catchment. The dashed field represents the Pb isotope and Pb content data in the of acid extracted matter in soil and sediment from a basalt watershed (Négrel and Roy, 2002b).

and Roy, 2002b), basalt and carbonate rock domains. The Pb isotope data in AEM (Fig. 8) are consistent with the Pb being derived from a mixture of granites and basalts, with both providing a roughly similar component. For basalts, Négrel and Roy (2002b) demonstrated the impact of atmospheric deposition and notably the input of Pb from gasoline, reflected by the high $^{207}Pb/^{206}Pb$ and $^{208}Pb/^{206}Pb$ values (Fig. 8). This finding points to a still existing reservoir for anthropogenic Pb in this watershed environment as a contaminant source and so precludes its direct use as a representative isotope ratio of the basalt-derived AEM. A regression for the AEM data from the Holocene sediment was performed using Isoplot (Ludwig, 2001) and shows a general trend passing from granites through Cretaceous carbonate rocks but the basalt rock domain does not occur within the relationship. A plot of error bar envelope shows that no account can be taken of the field of basalt rocks. This suggests mixing of more than two endmembers in varying proportions. From Figs. 7 and 8 it is clear that most of the Pb in AEM from the M25B core is derived from granite and basalt sources from the massif Central as well as some derivation of Pb from Jurassic carbonate rocks. The Pb isotope domain of Cretaceous carbonate rocks seems to be ruled out because it lies clearly inside the field of the Loire sediments and is unlikely to have contributed to the dispersion of the isotope data. However, the contribution from each of these sources is not quantifiable.

4.4. Lead inputs during the Holocene

Lead isotopes in the core of clayey channel infilling (Figs. 7 and 8) indicates types of bedrock as sources of Pb in the AEM. Lead mainly originated from the Massif Central but fluctuations of Pb content may reflect natural or human influenced inputs. Natural inputs are linked to landscape evolution in the Massif Central during the Holocene. One of the processes could be related to the latest period of volcanic events occurred from 11 to 3.45 ka BP (Aubert et al., 1973, Fig. 9). The volcanic activity was mainly located in the "Chaîne des Puys", area located in the Massif Central and drained by the Allier river. One of these events, namely the Vasset/Killian tephra dated at 8290±140 a BP (VKT, Aubert et al., 1973, Fig. 9), was recognised in lake sediments in Switzerland (Shotyk et al., 1998). The other natural inputs were mainly due to erosion processes of granites and basalts between the Bölling-Alleröd and Boreal periods, as evidenced by the variations in the sediment yield in a small watershed in the Massif Central (Macaire et al., 1997), which is part of the Loire catchment. Sediment yield during the Bölling-Alleröd

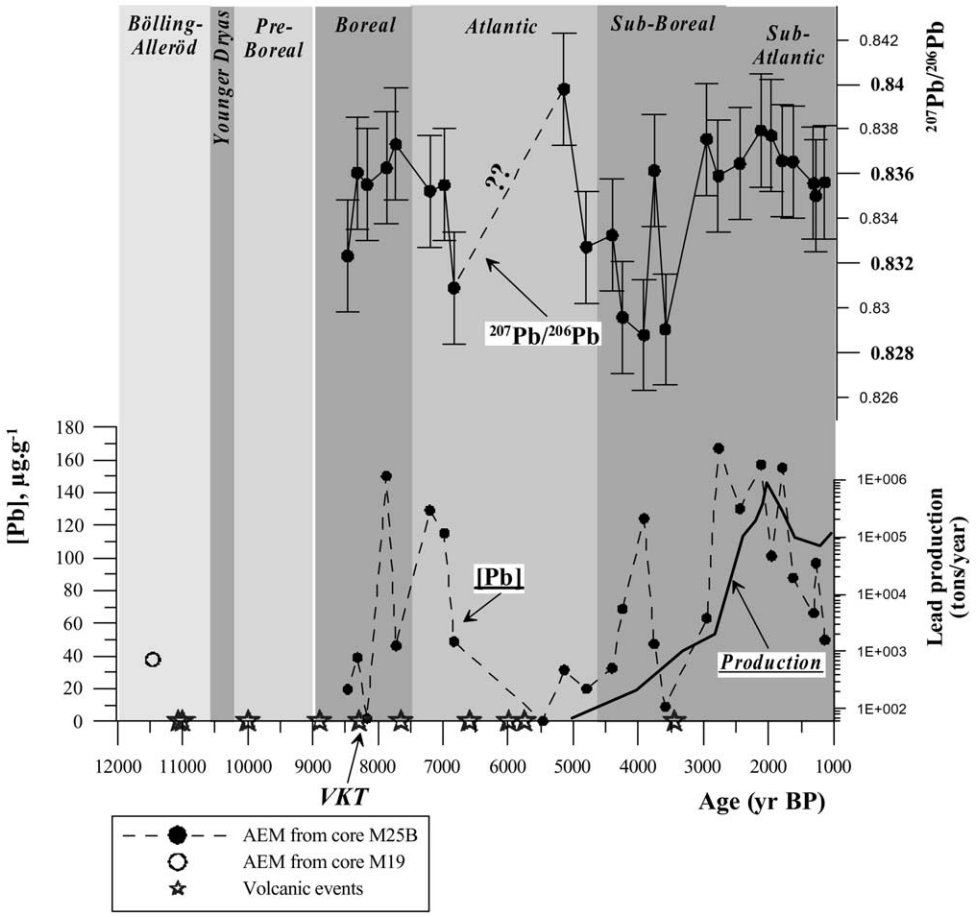

Fig. 9. $^{207}Pb/^{206}Pb$ isotopic ratio (upper dotted curve), Pb concentration (lower dotted curve) in AEM from core M25B, Pb production in the ancient world (full curve, see text) and volcanic events in the Massif Central (stars, see text); VKT corresponds to the Vasset/Killian tephra (Aubert et al., 1973).

period was rather low and may be explained by the temperate climate and the sparse woodland development (Beaulieu et al., 1988). A large increase in erosion during the Younger-Dryas period may be related to the colder climate and decline of the vegetation (Weiss et al., 1997; Shotyk et al., 2001). Sediment yield was similar during the pre-Boreal and Boreal periods. From the Atlantic to the Sub-Atlantic periods a large increase of the sediment yield was related by Beaulieu et al. (1988) and Macaire et al. (1997) to the influence of human activities. The landscape evolution during this period (burning, clearance for farming) is reflected in the vegetation patterns (Beaulieu et al., 1988). Human activities, associated with the humid temperate climate during this period would have enhanced the natural erosion rates.

As well as changing land use practices, another direct human influence on heavy metal budgets in the catchment was mining and smelting of ores. The history of Pb production began 5 ka BP by the discovery of techniques for smelting Pb–Ag ores (Settle and Patterson, 1980, Hong et al., 1994). The production of Pb increased continuously from 5 ka BP to a maximum at 2 ka BP during the Roman epoch (Fig. 9, Settle and Patterson, 1980). It then decreased during the decline of the Roman Empire to reach a minimum in medieval times. The smelter emissions caused atmospheric contamination which is recorded in Greenland ice cores (Hong et al., 1994; Rosman et al., 1997) and lake sediments (Germany, Sweden and Switzerland, Renberg et al., 1994, 2000; Weiss et al., 1997; Shotyk et al., 1998, 2001; Brännvall et al., 1999; Monna et al., 2000). In fact, an emission into the atmosphere of at least 5% of the mined Pb has been suggested (summary in Renberg et al., 1994). Spain was the most important region for Pb output during ancient times (Rosman et al., 1997; Martínez Cortizas et al., 2002) and Gaul represented only 6% of global Pb production (Rosman et al., 1997). The metalliferous mineralization in the Massif Central

comprise mainly Pb-bearing minerals and Sb-bearing minerals with Pb as a trace element (Marcoux, 1986), which were exploited during the Roman epoch (Vialaron, 1993).

Fig. 9 summarises the Pb isotopes and Pb contents in the M25B sediment record, the Pb production (Settle and Patterson, 1980) and the different volcanic events in the Massif Central during the Holocene (Aubert et al., 1973). The first maximum in Pb content occurring at 4.35 m depth (7.87 ka BP, Garcin et al., 2001; Fig. 8) coincides approximately with the VKT event dated 8290±140 a BP suggesting that part of Pb in AEM could have been affected either by direct deposition of VKT tephra or by erosion of the volcanic deposits. Moreover, the sediment yield during the Boreal was high (Macaire et al., 1997) and fresh volcanic deposits are well known to be rapidly weathered (Aubert et al., 1973; Louvat and Allègre, 1997). The influence of the VKT event was observed both in Pb contents and Pb isotopes in sediments in Switzerland (Shotyk et al., 1998). Similarly, such a Pb input in annually laminated sediments from Maar lakes in the West Eifel volcanic field (Germany) was shown by Schettler and Romer (1998). They showed an increase in the Pb content at 11.47 ka BP linked with the Ulmener Maar Tephra (UMT). However, the VKT influence in AEM from the M25B core is not clearly indicated by the $^{207}Pb/^{206}Pb$ ratio which remains around 0.83, which approaches the range of $^{207}Pb/^{206}Pb$ ratios (0.789–0.815) in basalts and is lower than that of granites (0.8405–0.863, see Section 4.3). It is worth noting that the VKT event influence was clearly evidenced in the sediments from Switzerland and not in the AEM from M25B core. This could be related to the large presence of basalt bedrocks in the Massif Central, still submitted to erosion processes in the Loire catchment, which is not the case in the lake catchments in Switzerland. For the latter, the influence of atmospheric deposition of particles emitted by the VKT event on the Pb isotope ratios was, de facto, more marked.

The second maximum in Pb content at 3.75–3.65 m depth (6.8–7.2 ka BP, Garcin et al., 2001) occurs soon after a volcanic event dated at 7650±350 a BP (Aubert et al., 1973). At these depths there is a shift toward lower $^{207}Pb/^{206}Pb$ ratios (0.8355–0.8309) that may reflect weathering of the basalts, but the duration of the shift is greater than for the VKT event. However, there is no evidence of an increase in Pb isotopes in sediments in Switzerland (Shotyk et al., 1998) or in Greenland ice cores (Rosman et al., 1997) at this time. This possibly implies either a more localised volcanic event or an increase in the erosion processes of basalts in the Massif Central.

The Pb content gradually increases up to 125 $\mu g.g^{-1}$ at 2.5 m depth (3.90 ka BP, Garcin et al., 2001), and the $^{207}Pb/^{206}Pb$ ratios also decrease from 0.8398 up to 0.8288. These decreases occur after a series of volcanic events dated from 6000±150 to 5750±150 a BP (Aubert et al., 1973). However, the duration of the increase in Pb contents and the decrease of the $^{207}Pb/^{206}Pb$ ratio is greater than can be explained by weathering of recent volcanic deposits alone. Both increases could also be related to human activities, such as forest burning and clearance for farming (Beaulieu et al., 1988), which cause increased erosion of soils. In any case, the erosion rate seems to be more marked in the basalts than in granites as the gradual decrease of the $^{207}Pb/^{206}Pb$ ratios suggests. A different explanation can be given for the latest increase in Pb contents that occurred after a volcanic event dated 3450±110 a BP. The increase of Pb content corresponds to an increase of the $^{207}Pb/^{206}Pb$ ratios. This period (e.g. late Sub-Boreal and the early Sub-Atlantic periods) corresponds to high overall Pb production in the ancient world, as demonstrated by Rosman et al. (1997) in Greenland ice by a decrease in the Pb isotope ratios in the period 3–2 ka BP. The concomitant fluctuations in Pb content and Pb isotope ratios could be related to the ore mining in the Massif Central (Vialaron, 1995) or by atmospheric deposition from mining activities in remote regions (Spain, Martínez Cortizas et al., 2002). The ends of the Sub-Boreal and the Sub-Atlantic periods are marked by a progressive decrease in Pb contents while the $^{207}Pb/^{206}Pb$ ratios display fluctuations from 0.8376 to 0.8356. A similar explanation (e.g. ore mining in the Massif Central and/or atmospheric deposition from mining activities in remote regions) can be given for the high and relatively constant Pb content in AEM during the period 2.4–1.7 ka BP. However, the Pb isotopic ratios of ore deposits in the Massif Central (Marcoux, 1986) are similar to those of granites in the Massif Central and of mineral veins in the Rio Tinto area (Rosman et al., 1997; Pomies et al., 1998; Martínez Cortizas et al., 2002). Therefore, the $^{207}Pb/^{206}Pb$ ratios in AEM around 0.836-0.838 at the same time are not consistent with Pb inputs from mining activities alone. A more likely explanation is a double origin for the Pb from erosion of soil on granites and basalts (natural plus human induced) and from mining activities. During the latest period, there was a decline of Pb production in the ancient world (Settle and Patterson, 1980) and the fluctuations in the $^{207}Pb/^{206}Pb$ ratio in the uppermost part of the M25B core could have resulted from the weathering of granites and basalts alone.

The present results agree with the work of Alfonso et al. (2003) on Pb content and Pb isotope ratios in bulk sediment samples in cores covering the last 6 ka from marshes in south-western France. The evolution of the Pb isotope ratio they highlighted reveals a good correlation with world-wide Pb production during the last 5 ka. More precisely, the lead isotopic records reveal some general trends, along with a few typical events such as the imprints of the pre-anthropogenic background (6 to

2.3 ka BP), the mining activity during the Roman and Greek periods (2.3 to 1.7 ka BP) as well as the fall of the Roman Empire (see also Renberg et al., 2000, 2002). Schettler and Romer (1998) also found evidence in the sediments from Maar lakes in the West Eifel volcanic field (Germany) of anomalously high Pb within sections deposited during the first centuries A.D. Lead content, exceeding the local geological background, causing the anomaly has the same isotopic composition as galena deposits located in the vicinity of the Maar lakes and they suggested that the excess Pb originated from regional Roman Pb refining and cupellation of Pb ores.

Lead content and Pb isotope data provide useful markers in riverine sedimentary records. Lead originated from the granite and basalts of the Massif Central, through erosion processes' and from mining activities but the fluvially transported material should give a mean for Pb dispersion, as Négrel et al. (2002) found with Sr isotopes.

5. Conclusions

In the clayey channel infilling of the alluvial plain of the Middle Loire River (France), which covers the period from the Boreal to the Sub-Atlantic, Mn, V and Pb are negatively correlated with the amount of AEM in the sediments. Because the AEM is closely related to calcite contents; it can be concluded that the principal carrier phase for the metals is part of the non-carbonate fraction, probably the Fe–Mn oxy-hydroxides and organic matter. The correlations of Mn, and Pb with V and Th as a typical indicator of crustal weathering points to their derivation from the crystalline basement of the upper part of the catchment (Massif Central) or from volcanic rocks in the same area. The trace element contents of the small amount of carbonate in the AEM are similar to those of the Aquitanian lacustrine limestone.

The hypothesis that AEM contributions result from crustal weathering are confirmed by the Pb isotope ratios in the late Holocene Loire sediments. Most of the Pb is derived from the crystalline basement and volcanic intrusions of the Massif Central and carbonate contributes little. As there are few Pb isotope data for French carbonate rocks, the nature of the carbonate endmember remains hypothetical. Further evidence for the origin of the carbonate fraction is expected to arise from the interpretation of C and O stable isotope data from the same samples of the Loire alluvial sediment sequence.

Fluctuations in Pb content and isotopic composition were probably related to either natural inputs (erosion processes, volcanic events) or human impacts (burning and clearance of forest for agriculture, and mining and smelting of Pb ore) during the Holocene. Volcanic events such as the Vasset/Killian tephra event are recorded in the AEM of the sediment core. However, the duration of increases in Pb contents and the $^{207}Pb/^{206}Pb$ ratio variations were sometimes greater than can be explained by weathering of recent volcanic deposits alone. Increased erosion as the result of soil cultivation in the mid to late Holocene may have prolonged the contribution of volcanic material to the alluvial deposits. In the late Sub-Boreal and the Sub-Atlantic periods the Pb originated from weathering of granites and basalts (natural plus human induced) and from ore mining.

Acknowledgements

This work was financially supported by the program "Morphogénèse Fluviale" within the BRGM Research Division. Analyses of trace elements and Pb isotopes were performed at the joint BRGM-INSU-CEA laboratory at Saclay (France). We are grateful to R. Harmon for thoughtful comments and constructive remarks. We have benefited from the constructive comments and thoughtful revisions of the manuscript by L. Neymark, S. Chenery and J. Ridgway.

References

Aiuppa, A., Allard, P., D'Allessandro, W., Michel, A., Parello, F., Treuil, M., Valenza, M., 2000. Mobility and fluxes of major, minor and trace metals during basalt weathering and groundwater transport at Mt Etna volcano (Sicily). Geochim. Cosmochim. Acta 64, 1827–1841.

Alfonso, S., Grousset, F., Massé, L., Tastet, J.P., 2003. A European lead isotope signal recorded from 6000 to 300 years BP in coastal marshes (SW France). Atmos. Environ. 35, 3595–3605.

Aubert, M., Bouiller, R., Camus, G., Cochet, A., D'Arcy, D., Giot, D., Jeambrun, M., Roche, A., Bonhommet, N., 1973. Carte géologique à l'échelle du 1/50000, feuille Clermont-Ferrand XXV631. Notice, BRGM ed.

de Beaulieu, J.L., Pons, A., Reille, M., 1988. Histoire de la végétation, du climat et de l'action de l'homme dans le Massif Central français depuis 15 000 ans. Inst. Fr. Pondichéry, Trav. sec. Sci. Tech. XXV, 27–32.

BRGM., 1996. Carte géologique de la France au 1/1.000.000, 6ème édit.

Brännvall, M.L., Bindler, R., Renber, I., Emteryd, O., Bartnicki, J., Billström, K., 1999. The medieval metal industry was the cradle of modern large-scale atmospheric lead pollution in northern Europe. Environ. Sci. Technol. 33, 4391–4395.

Brown, G., 1961. The X-Ray Identification and Crystal Structures of Clay Minerals. Mineral Society, London.

Calvert, S.E., Piper, D.Z., 1974. Geochemistry of ferromanganese nodules from DOMES Sites A, Northern equatorial Pacific: Multiple diagenetic metal source in the deep sea. Geochim. Cosmochim. Acta 50, 2467–2479.

Cocherie, A., Négrel, Ph., Roy, S., Guerrot, C., 1998. Direct determination of Pb/Pb isotopic ratios in rainwater using ICP-MS. J. Anal. Atom. Spect. 13, 1069–1073.

Chester, R., Kudoja, W.M., Thomas, A., Towner, J., 1985. Pollution reconnaissance in stream sediments using non-residual trace metals. Environ. Pollut. 10, 213–238.

Dong, D., Derry, L.A., Lion, L.W., 2003. Pb scavenging from a freshwater lake by Mn oxides in heterogeneous surface coating materials. Water Res. 37, 1662–1666.

Downes, H., Shaw, A., Williamson, B.J., Thirlwall, M.F., 1997. Sr, Nd, Pb in Hercynian granodiorites and monzogranites, Massif Central, France. Chem. Geol. 136, 99–122.

Emmanuel, S., Erel, Y., 2002. Implications from concentrations and isotopic data for Pb partitioning processes in soils. Geochim. Cosmochim. Acta 66, 2517–2527.

Faure, G., 1986. Principles of Isotope Geology. John Wiley and Sons.

Fiszman, M., Pfeiffer, W.C., Drude de Lacerda, L., 1984. Comparison of methods used for extraction and geochemical distribution of heavy metals in bottom sediments from Sepetiba Bay (Brazil). Environ. Technol. Lett. 5, 567–575.

Gaillardet, J., Dupre, B., Allègre, C.J., Négrel, Ph., 1997. Chemical and physical denudation in the Amazon river basin. Chem. Geol. 142, 141–173.

Gaillardet, J., Dupré, B., Allègre, C.J., 1999. Geochemistry of large river suspended sediments: Silicate weathering or recycling tracer? Geochim. Cosmochim. Acta 63, 4037–4051.

Garcin, M., Giot, D., Farjanel, G., Gourry, J.-C., Kloppmann, W., Négrel, Ph., 1999. Tardiglacial and Holocene deposits in the Middle Loire River, the Val d'Avaray case study (Loir et Cher, France). C. R. Acad. Sci. IIA 329, 405–412.

Garcin, M., Giot, D., Farjanel, G., 2001. Radiocarbon dating and palynology of alluvial deposits in the Loire flood plain (Val d'Avaray, Loir et Cher, France). Quaternaire 12.

Grosbois, C., Négrel, P., Fouillac, C., Grimaud, D., 2000. Chemical and isotopic characterization of the dissolved load of the Loire river. Chem. Geol. 170, 179–201.

Grousset, F.E., Quetel, C.R., Thomas, B., Buat-Menard, P., Donard, O.F.X., Bucher, A., 1994. Transient Pb isotopic signatures in the Western European atmosphere. Environ. Sci. Technol. 28, 1605–1608.

Hansmann, W., Köppel, V., 2000. Lead isotopes as tracers of pollutants in soils. Chem. Geol. 171, 123–144.

Hinrichs, J., Dellwig, O., Brumsack, H.J., 2002. Lead in sediments and suspended particulate matter of the German Bight: natural versus anthropogenic origin. Appl. Geochem. 17, 621–632.

Hong, S., Candelone, J.P., Patterson, C.C., Boutron, C.F., 1994. Greenland ice evidence of hemispheric lead pollution two millennia ago by Greek and Roman civilizations. Science 265, 1841–1843.

Hopper, J.F., Ross, H.B., Sturges, W.T., Barrie, L.A., 1991. Regional source discrimination of atmospheric aerosols in Europe using the isotopic composition of lead. Tellus 43B, 45–60.

Hotzapssel, T., 1985. Les minéraux argileux. Préparation. Analyse diffractométrique et détermination. Société Géologique du Nord, 12.

Langmuir, D., Herman, J.S., 1980. The mobility of thorium in natural waters at low temperatures. Geochim. Cosmochim. Acta 44, 1753–1766.

Leleyter, L., Probst, J.L., 1999. A new sequential extraction procedure for the speciation of particulate trace elements in river sediments. Internat. J. Environ. Anal. Chem. 73, 109–128.

Louvat, P., Allègre, C.J., 1997. Present denudation rates on the island of Reunion determined by river geochemistry: basalt weathering and mass budget between chemical and mechanical erosions. Geochim. Cosmochim. Acta 61, 3645–3669.

Luck, J.M., BenOthman, D., 1998. Geochemistry and water dynamics. II. Trace metals and Pb-Sr isotopes as tracers of water movements and erosion processes. Chem. Geol. 150, 263–282.

Ludwig, K.R., 2001. Users manual for ISOPLOT/EX, version 2.49. A geochronological toolkit for Microsoft Excel. Berkeley Geochronology Center. Spec. Publ. 1a.

Macaire, J.J., Bossuet, G., Choquier, A., Cocirta, C., De Luca, P., Dupis, A., Gay, I., Mathey, E., Guenet, P., 1997. Sediment yield during late glacial and Holocene periods in the Lac Chambon watershed, Massif Central, France. Earth Surf. Proc. Landforms 22, 473–489.

MacKenzie, A.B., Pulford, I.D., 2002. Investigation of contaminant metal dispersal from a disused mine site at Tyndrum, Scotland, using concentration gradients and stable Pb isotope ratios. Appl. Geochem. 17, 1093–1103.

Marcoux, E., 1986. Isotopes du plomb et paragénèses métalliques, traceurs de l'histoire des gîtes minéraux. Illustration des concepts de sources, d'héritage et de régionalisme dans les gîtes français, application en recherche minière. Thèse d'état, Univ. Clermont-Ferrand, Document du BRGM, 117.

Martínez Cortizas, A., García-Rodeja, E., Pontevedra Pombal, X., Nóvoa Muñoz, J.C., Weiss, D., Cheburkin, A., 2002. Atmospheric Pb deposition in Spain during the last 4600 years recorded by two ombrotrophic peat bogs and implications for the use of peat as archive. Sci. Total Environ. 292, 33–44.

Meade, R.H., 1988. Movement and storage of sediment in river systems. In: Lerman, A., Meybeck, M. (Eds.), Physical and Chemical Weathering in Geochemical Cycles. Kluwer Academic Pub, Dordrecht, pp. 165–180.

Meade, R.H., Yuzyk, T.R., Day, T.J., 1990. Movement and storage of sediment in rivers of the United States and Canada. In The Geology of North America, Surface Water Hydrology. Geol. Soc. America, pp. 255–280.

Michard-Vitrac, A., Albarede, F., Allègre, C.J., 1981. Lead isotopic composition of Hercynian granitic K-feldspars constrains continental genesis. Nature 291, 460–464.

Monna, F., Lancelot, J., Croudace, I.W., Cundy, A.B., Lewis, J.T., 1997. Pb isotopic composition of airborne particulate material from France and the Southern United Kingdom: implications for Pb pollution sources in urban areas. Environ. Sci. Technol. 31, 2277–2286.

Monna, F., Dominik, J., Loizeau, J.L., Pardos, M., Arpagaus, P., 1999. Origin and evolution of Pb in sediments of Lake Geneva (Switzerland- France). Establishing a stable Pb record. Environ. Sci. Technol. 33, 2850–2857.

Monna, F., Hamer, K., Lévêque, J., Sauer, M., 2000. Pb isotopes as a reliable marker of early mining and smelting in the northern Harz province (Lower Saxony, Germany). J. Geochem. Expl. 68, 201–210.

Morford, J.L., Emerson, S., 1999. The geochemistry of redox sensitive trace metals in sediments. Geochim. Cosmochim. Acta 63, 1735–1750.

Mukai, H., Tanaka, A., Fujii, T., Nakao, H., 1994. Lead isotope ratios of airborne particulate matter as tracers of long range transport of air pollutants around Japan. J. Geophys. Res. 99, 3717–3726.

Négrel, Ph., Grosbois, C., 1999. Changes in distribution patterns of chemical elements and $^{87}Sr/^{86}Sr$ isotopic signatures in suspended matter and bed sediments transported out by the upper Loire River watershed (France). Chem. Geol. 156, 231–249.

Négrel, Ph., Grosbois, C., Kloppmann, W., 2000. The labile fraction of suspended matter in the Loire river (France): multi-element chemistry and isotopic (Rb-Sr and C-O) systematics. Chem. Geol. 166, 271–285.

Négrel, Ph., Kloppmann, W., Garcin, M., Giot, D., 2002. Strontium isotopic record of signatures of Holocene fluvial sediments in the Loire valley, France. Hydrol. Earth System Sci. 6, 849–858.

Négrel, Ph., Roy, S., 2002a. Tracing the sources of the labile fraction in fluvial sediments by trace elements and strontium isotopes. In: Bousmar, D., Zech, Y. (Eds.), Proc. Internat. Conf. Fluvial Hydraulics, Riverflow 2002, Belgium. Balkema, Lisse, pp. 1129–1134.

Négrel, Ph., Roy, S., 2002b. Investigating the sources of the labile fraction in sediments from silicate-drained rocks using trace elements, and strontium and lead isotopes. Sci. Total Environ. 298, 163–182.

Outridge, P.M., Hermanson, M.H., Lockhart, W.L., 2002. Regional variations in atmospheric deposition and sources of anthropogenic lead in lake sediments across the Canadian Arctic. Geochim. Cosmochim. Acta 66, 3521–3531.

Pomies, C., Cocherie, A., Guerrot, C., Marcoux, E., Lancelot, J., 1998. Assessment of the precision and accuracy of lead-isotope ratios measured by TIMS for geochemical applications: example of massive sulphide deposits (Rio Tinto, Spain). Chem. Geol. 144, 137–149.

Renberg, I., Persson, M.W., Emteryd, O., 1994. Pre-industrial atmospheric lead contamination detected in Swedish lake sediments. Nature 368, 323–326.

Renberg, I., Brännvall, M.L., Bindler, R., Emteryd, O., 2000. Atmospheric lead pollution history during four millenia (2000 BC to 2000 AD) in Sweden. Ambio 29, 150–156.

Renberg, I., Brännvall, M.L., Bindler, R., Emteryd, O., 2002. Stable lead isotopes and lake sediments—a useful combination for the study of atmospheric lead pollution history. Sci. Total Environ. 292, 45–54.

Robinson, G.D., 1993. Major element chemistry and micromorphology of Mn-oxides coatings on stream alluvium. Appl. Geochem. 8, 633–642.

Rosman, K.J.R., Chisholm, W., Hong, S., Candelone, J.P., Boutron, C.F., 1997. Lead from Carthaginian and Roman Spanish mines isotopically identified in Greenland ice dated from 600 B.C. to 300 A.D. Environ. Sci. Technol. 31, 3413–3416.

Roy, S., 1996. Utilisation des isotopes du Pb et du Sr comme traceurs des apports anthropiques et naturels dans les précipitations et les rivières du Bassin de Paris. PhD thesis, Univ. Paris 7.

Schettler, G., Romer, R.L., 1998. Anthropogenic influences on Pb/Al and lead isotope signature in annually layered Holocene Maar lake sediments. Appl. Geochem. 13, 787–797.

Schiller, A.M., Mao, L., 2000. Dissolved V in rivers: effects of silicate weathering. Chem. Geol. 165, 13–22.

Settle, D.M., Patterson, C.C., 1980. Lead in Albacore: Guide to lead pollution in Americans. Science 207, 1167–1176.

Shotyk, W., Weiss, D., Appleby, P.G., Frei, R., Gloor, M., Kramers, J.D., Reese, S., Van Der Knaap, W.O., 1998. History of atmospheric lead deposition since 12,370 ^{14}C yr BP from a peat bog, Jura Mountains, Switzerland. Science 281, 1635–1640.

Shotyk, W., Weiss, D., Kramers, J.D., Frei, R., Cheburkin, A.K., Gloor, M., Reese, S., 2001. Geochemistry of the peat bog at Etang de la Gruère, Jura Mountains, Switzerland, and its record of atmospheric Pb and lithogenic trace metals (Sc, Ti, Y, Zr, and REE) since 12,370 ^{14}C yr BP. Geochim. Cosmochim. Acta 65, 2337–2360.

Sposito, G., 1989. The Chemistry of Soils. Oxford University Press.

Sutherland, R.A., 2002. Comparison between non-residual Al, Co, Cu, Fe, Mn, Ni, Pb and Zn released by a three-step sequential extraction procedure and a dilute hydrochloric acid leach for soil and road deposited sediment. Appl. Geochem. 17, 353–365.

Sutherland, R.A., Day, J.P., Bussen, J.O., 2003. Lead concentrations, isotope ratios, and source apportionment in road deposited sediments, Honolulu, Oahu, Hawaii. Water Air Soil Poll. 142, 165–186.

Teutsch, N., Erel, Y., Halicz, L., Banin, A., 2001. Distribution of natural and anthropogenic lead in Mediterranean soils. Geochim. Cosmochim. Acta 65, 2853–2864.

Vialaron, Ch., 1993. L'antimoine dans le département de la Haute-Loire (Antimony in the Haute-Loire District, in French), Vialaron Ch. ed., Clermont-Ferrand, France.

Wehrli, B., Stumm, W., 1989. Vanadyl in natural waters: adsorption and hydrolysis promote oxygenation. Geochim. Cosmochim. Acta 53, 69–77.

Weiss, D., Shotyk, W., Cherbukin, A.K., Gloor, M., Reese, S., 1997. Atmospheric lead deposition from 12,400 to ca. 2000 yrs BP in a peat bog profile, Jura Mountains, Switzerland. Water Air Soil Poll. 100, 311–324.